Four Molecular Superconductors Isolated as Nanoparticles

Dominique de Caro, C. Faulmann, Lydie Valade, Kane Jacob, Imane Chtioui, Soukaina Foulal, Pascale Satgé-de Caro, Manon Bergez-Lacoste, Jordi Fraxedas, Belén Ballesteros, et al.

DOI:10.1002/ejic.201402007

Four Molecular Superconductors Isolated as Nanoparticles

Dominique de Caro,*[a,b] Christophe Faulmann,*[a,b] Lydie Valade,[a,b] Kane Jacob,[a,b] Imane Chtioui,[a,b] Soukaina Foulal,[a,b] Pascale de Caro,[c,d] Manon Bergez-Lacoste,[c,d] Jordi Fraxedas,[e] Belén Ballesteros,[e] James S. Brooks,[f] Eden Steven,[f] and Laurel E. Winter[f]

Keywords: Nanoparticles / Superconductors / Electrochemistry / Ionic liquids / Bechgaard salts

$(TMTSF)_2PF_6$ and $(TMTSF)_2ClO_4$ Bechgaard salts, $(BEDT\text{-}TTF)_2I_3$, and $TTF[Ni(dmit)_2]_2$ [TMTSF = tetramethyltetraselenafulvalene; BEDT-TTF = bis(ethylenedithio)tetrathiafulvalene; TTF = tetrathiafulvalene; dmit = 1,3-dithiole-2-thione-4,5-dithiolate] are among the most popular molecular superconductors. They are grown as nanoparticles that exhibit properties in agreement with those of the bulk. The shape, size, and homogeneity of particles depend on the stabilizing agent and synthesis conditions. We report on the more recent conditions investigated (i) to produce nanoparticles of 35 nm for β-$(BEDT\text{-}TTF)_2I_3$, (ii) to reduce the particle size to 10–15 nm for $TTF[Ni(dmit)_2]_2$ and 3–5 nm for $(TMTSF)_2ClO_4$, and (iii) to improve the growth duration from days to one hour for $(TMTSF)_2PF_6$. Finally, we report evidence of superconductivity in $(TMTSF)_2ClO_4$ particles.

Introduction

The four molecular superconductors $(TMTSF)_2PF_6$ and $(TMTSF)_2ClO_4$ Bechgaard salts, $(BEDT\text{-}TTF)_2I_3$, and $TTF[Ni(dmit)_2]_2$ [TMTSF = tetramethyltetraselenafulvalene; BEDT-TTF = bis(ethylenedithio)tetrathiafulvalene; dmit = 1,3-dithiole-2-thione-4,5-dithiolate] (Scheme 1) were first prepared in the 1980s and 1990s.[1] They are the parent compounds of a well-known series of superconductors and can be taken as models for studying the influence of morphology and size on physical properties, for instance, on the occurrence of superconductivity. We have explored the preparation of these compounds as thin films[1] and as nanoparticles (NPs).[2] $(BEDT\text{-}TTF)_2I_3$ was also studied as a composite film.[3] In particular, superconductivity was evidenced in thin films of $TTF[Ni(dmit)_2]_2$,[4] $(TMTSF)_2ClO_4$,[5] and $(BEDT\text{-}TTF)_2I_3$.[6] Preparing molecular conductors as thin films or nanoparticles follows the ultimate goal of integrating them into electronic devices. In this case, the materials are selected for their room-temperature properties. Therefore, research focuses on their preparation in forms transferable onto surfaces, and on the study of the consequences of the final morphology on physical properties. For example, colloidal solutions of TTF-TCNQ NPs (TCNQ = tetracyanoquinodimethane) offer promising applications,[7] a chemistry-based technique for patterning films of $(BEDT\text{-}TTF)_2I_3$ on a polymeric substrate was described,[8] and surface-selective deposition of TTF-TCNQ, $TTF[Ni(dmit)_2]_2$, and $(BEDT\text{-}TTF)_2I_3$ NPs was applied to the construction of organic transistor structures.[2b]

[a] CNRS, LCC (Laboratoire de Chimie de Coordination), 205 route de Narbonne, BP 44099, 31077 Toulouse Cedex 4, France
E-mail: dominique.decaro@lcc-toulouse.fr
christophe.faulmann@lcc-toulouse.fr
www.lcc-toulouse.fr
[b] Université de Toulouse, UPS, INPT, 31077 Toulouse Cedex 4, France
[c] Université de Toulouse, INPT-ENSIACET, LCA (Laboratoire de Chimie Agro-industrielle), 31030 Toulouse, France
[d] INRA, UMR 1010 CAI, 31030 Toulouse, France
[e] Institut Catala de Nanociencia i Nanotecnologia (ICN2) and Consejo Superior de Investigaciones Científicas (CSIC), Campus UAB, 08193 Bellaterra, Spain
[f] NHMLF/Physics, Florida State University, Tallahassee, FL 32310, USA

Supporting information for this article is available on the WWW under http://dx.doi.org/10.1002/ejic.201402007.

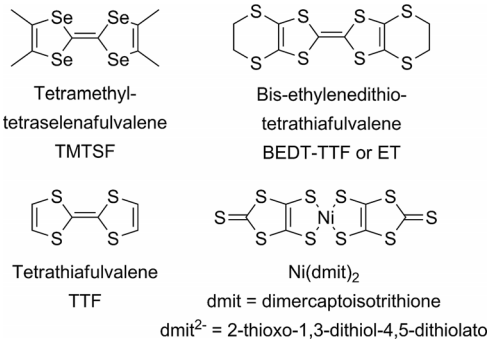

Scheme 1. Molecular building blocks of $(TMTSF)_2PF_6$, $(TMTSF)_2ClO_4$, $(BEDT\text{-}TTF)_2I_3$, and $TTF[Ni(dmit)_2]_2$ superconductors.

By taking advantage of our previous work, we investigated the preparation of NPs of β-(BEDT-TTF)$_2$I$_3$ and developed new conditions for the preparation of NPs of TTF[Ni(dmit)$_2$]$_2$, (TMTSF)$_2$PF$_6$, and (TMTSF)$_2$ClO$_4$ to produce smaller homogeneous particles (Table 1) and to perform physical studies to provide evidence of their superconductivity. We report the preparation and study of NPs of β_{CO}-(BEDT-TTF)$_2$I$_3$ (CO stands for "chemical oxidation") obtained following an iodine chemical oxidation of BEDT-TTF[1,9] in the presence of the ionic liquid (IL) (BMIM)[N(CF$_3$SO$_2$)$_2$] (Scheme 2). We describe the preparation of TTF[Ni(dmit)$_2$]$_2$ NPs at room temperature using an electrochemical procedure in the presence of (BMIM)[N(CF$_3$SO$_2$)$_2$]. (TMTSF)$_2$PF$_6$ and (TMTSF)$_2$ClO$_4$ NPs were prepared by electrolysis as previously reported.[2a] In this work, we investigate the influence of the growth speed on the size and morphology of (TMTSF)$_2$PF$_6$ NPs, and of the addition of neutral long-chain molecules to the ammonium salts *n*Bu$_4$NClO$_4$ and [Me(*n*-Oct)$_3$N]ClO$_4$ on the formation of (TMTSF)$_2$ClO$_4$ NPs. Finally, we present the preliminary physical studies that show the occurrence of superconductivity in (TMTSF)$_2$ClO$_4$ NPs.

Table 1. Synthesis conditions of β_{CO}-(BEDT-TTF)$_2$I$_3$, TTF[Ni(dmit)$_2$]$_2$, (TMTSF)$_2$PF$_6$, and (TMTSF)$_2$ClO$_4$ nanoparticles. All experiments were performed at room temperature by following electrochemical procedures unless otherwise specified (see the Exp. Section for details).

Precursors and stabilizers	Solvent	Current intensity duration	Characteristics of product
BEDT-TTF	THF	chemical procedure at 85 °C	NPs
I_2 (BMIM)[N(CF$_3$SO$_2$)$_2$]			35 nm
TTF *n*Bu$_4$N[Ni(dmit)$_2$] (BMIM)BF$_4$	CH$_3$CN	150 μA/24 h	NPs 15–20 nm
TTF *n*Bu$_4$N[Ni(dmit)$_2$] (BMIM)[N(CF$_3$SO$_2$)$_2$]	CH$_3$CN	80 μA/24 h	nanosticks 15–20 nm
TTF *n*Bu$_4$N[Ni(dmit)$_2$] (BMIM)[N(CF$_3$SO$_2$)$_2$]	CH$_3$CN	500 μA/4 h	NPs 10–15 nm
TMTSF (BMIM)PF$_6$	CH$_2$Cl$_2$	10 μA/72 h	NPs 30–50 nm
TMTSF (BMIM)PF$_6$	CH$_2$Cl$_2$	200 μA 3 h 50	NPs 50 nm
TMTSF (BMIM)PF$_6$	CH$_2$Cl$_2$	500 μA 1 h 15	NPs 55 nm
TMTSF [Me(*n*-Oct)$_3$N]ClO$_4$	CH$_2$Cl$_2$	10 μA/3 d	NPs 25–35 nm
TMTSF *n*Bu$_4$NClO$_4$ hexadecylamine	THF	10 μA/3 d	NPs 35 nm
TMTSF *n*Bu$_4$NClO$_4$ dodecylamine	THF	10 μA/3 d	NPs 40–65 nm
TMTSF (*n*Bu$_4$N)ClO$_4$ *n*-octylamine	THF	10 μA/3 d	NPs 35–70 nm
TMTSF *n*Bu$_4$NClO$_4$ methyl oleate	THF	10 μA/3 d	NPs 20–60 nm
TMTSF *n*Bu$_4$NClO$_4$ *N*-octylfurfurylimine	THF	10 μA/3 d	NPs 20–60 nm
TMTSF *n*Bu$_4$NClO$_4$ *N*-octylfuran-2-carboxamide	THF	10 μA/3 d	NPs 20–60 nm
TMTSF [Me(*n*-Oct)$_3$N]ClO$_4$ hexadecylamine	CH$_2$Cl$_2$	40 μA/20 h	NPs 20–50 nm

1-butyl-3-methylimidazolium

BMIM$^+$; X$^-$ = BF$_4^-$, [N(CF$_3$SO$_2$)$_2$]$^-$

Scheme 2. Ionic liquids used for growth control of nanoparticles.

Results and Discussion

β_{CO}-(BEDT-TTF)$_2$I$_3$ Nanoparticles

BEDT-TTF afforded the largest number of superconducting phases that exhibited various structural arrangements depending on the associated anions. The superconductor (BEDT-TTF)$_2$I$_3$ can adopt the three well-known β-, θ-, and κ-type modifications.[1,10] All of them show superconducting transitions at ambient pressure.[11] Nanocrystals of α- and β-(BEDT-TTF)$_2$I$_3$ were observed in thin films as embedded in a polycarbonate matrix[12] and in core–shell-type nanocomposite NPs of α-(BEDT-TTF)$_2$I$_3$ in which the nanocrystals act as shell layers and as the binder in aggregated silica particles.[13] Core–shell highly dispersed NPs that consist of the molecular conductor as the core material and the stabilizing agent as the shell layer can be isolated by using appropriate stabilizing agents. Polyvinylpyrrolidone (PVP) (Scheme 3) was successfully used to prepare NPs of (BEDT-TTF)$_2$I$_3$.[2b] We have investigated the use of the ionic liquid (IL) (BMIM)[N(CF$_3$SO$_2$)$_2$] as the stabilizing agent.

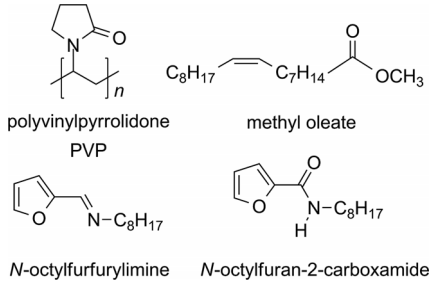

polyvinylpyrrolidone PVP — methyl oleate

N-octylfurfurylimine — *N*-octylfuran-2-carboxamide

Scheme 3. Polymers used for growth control of nanoparticles.

β_{CO}-(BEDT-TTF)$_2$I$_3$ NPs were prepared by chemical oxidation of BEDT-TTF by iodine, using a procedure previously reported[1,9] and in the presence of

(BMIM)[$N(CF_3SO_2)_2$]. Relative to previously isolated nanomaterials based on (BEDT-TTF)$_2I_3$, this procedure affords well-dispersed NPs with an average size of 35 nm as observed by TEM (Figure 1). X-ray diffraction, and Raman and IR spectroscopy confirm the formation of β_{CO}-(BEDT-TTF)$_2I_3$ (see Figures S1–S3 in the Supporting Information). The room-temperature conductivity of the NP powders, measured on a compacted pellet, is 1.5 S cm^{-1}. This value is consistent with the respective contributions to the conductivity: the intrinsic conductivity of NPs, resistance owing to the IL shell around NPs, and NP boundaries.

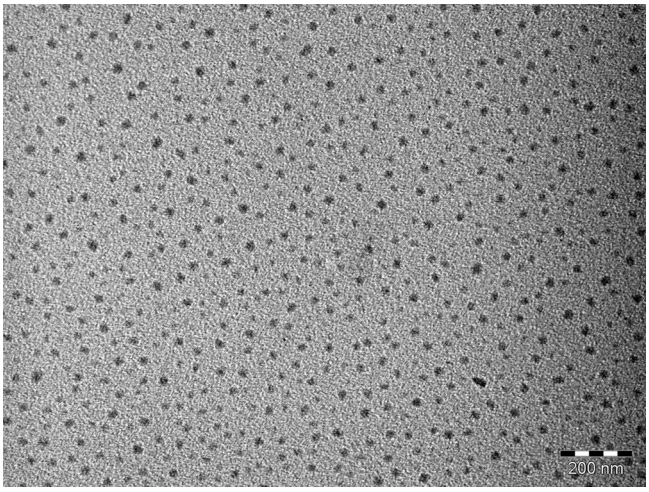

Figure 1. Electron micrographs for β_{CO}-(BEDT-TTF)$_2I_3$ with (BMIM)[$N(CF_3SO_2)_2$]; scale bar: 200 nm.

TTF[Ni(dmit)$_2$]$_2$ Nanoparticles

The [Ni(dmit)$_2$] molecule afforded the first series of superconductors that contain a transition-metal complex as the acceptor building block. The series opened with the TTF[Ni(dmit)$_2$]$_2$ compound that exhibited a room-temperature conductivity of 300 S cm^{-1} and a T_c at 1.6 K under an applied hydrostatic pressure of 7 kbar.[14] The phase diagram of this compound was additionally investigated recently.[15] The preparation of thin films, nanowires, and nanoparticles of TTF[Ni(dmit)$_2$]$_2$ was investigated,[16] and superconductivity was evidenced in electrodeposited films.[4] Previously synthesized NPs of TTF[Ni(dmit)$_2$]$_2$ were prepared using a chemical procedure that involved the reaction of (TTF)$_3$(BF$_4$)$_2$ with nBu$_4$N[Ni(dmit)$_2$].[2a,16b] The best results in terms of shape, dispersion, and homogeneity of the NPs were obtained in the presence of (BMIM)BF$_4$ or (BMIM)[$N(CF_3SO_2)_2$] and at –80 °C. These conditions afford particles of 30 nm (Figure 2, a). When this chemical procedure was conducted at room temperature, fewer NPs were produced and they were irregular, aggregated, or elongated. When TTF was electrochemically oxidized in the presence of nBu$_4$N[Ni(dmit)$_2$] and either (BMIM)BF$_4$ or (BMIM)[$N(CF_3SO_2)_2$], well-dispersed NPs of TTF[Ni(dmit)$_2$]$_2$ were produced at room temperature. TEM observations show nanoparticles of 15–20 and 10–15 nm in (BMIM)BF$_4$ and (BMIM)[$N(CF_3SO_2)_2$], respectively (Figure 2, b and c). The electrochemical procedure afforded smaller nanoparticles at room temperature than those from the chemical procedure. Additionally, the process is more efficient in producing nanoparticles at high current density: nanosticks were preferred when the electrolysis was conducted for 24 h at 80 μA and nanoparticles were obtained at 500 μA for 4 h. IR and Raman spectroscopy confirm the formation of TTF[Ni(dmit)$_2$]$_2$ (see Figures S4 and S5 in the Supporting Information). The conductivity was measured on a compacted pellet of NPs powder and found to be 0.5 S cm^{-1}, which was consistent with powdered samples.

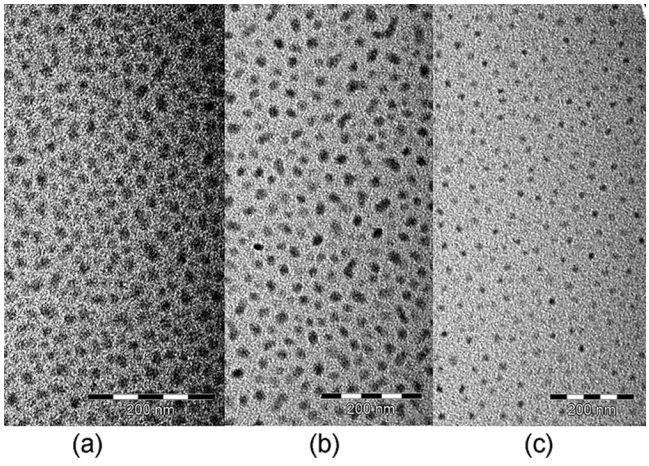

Figure 2. Electron micrographs for TTF[Ni(dmit)$_2$]$_2$ with (a) chemical procedure, (BMIM)BF$_4$, –80 °C; (b) electrochemical procedure, (BMIM)BF$_4$; and (c) electrochemical procedure, (BMIM)-[$N(CF_3SO_2)_2$]. Scale bar: 200 nm.

(TMTSF)$_2$PF$_6$ Nanoparticles

(TMTSF)$_2$PF$_6$ belongs to the so-called Bechgaard salts that led to the first organic superconducting phases. (TMTSF)$_2$PF$_6$ undergoes a superconductive transition at

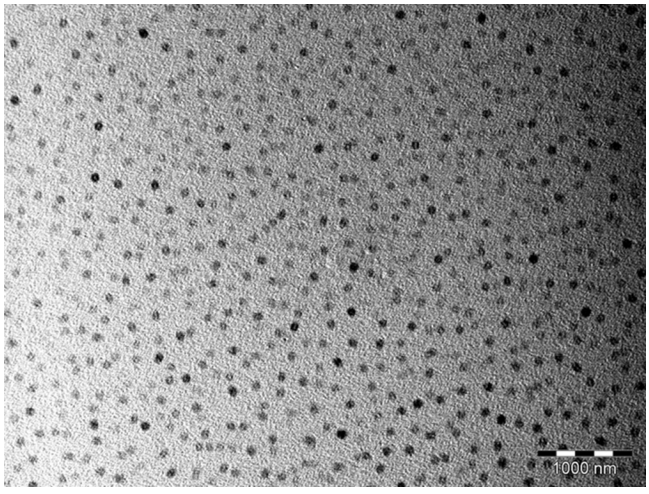

Figure 3. Electron micrograph for (TMTSF)$_2$PF$_6$ with (BMIM)PF$_6$ at 500 μA; scale bar: 1000 nm.

0.9 K under a pressure of 12 kbar.[17] NPs of $(TMTSF)_2PF_6$ have previously been isolated by electrolysis in the presence of $(BMIM)PF_6$, which acts as both the supporting electrolyte and the stabilizer.[18] We have followed similar concentration conditions (TMTSF/IL = 1:10) and have investigated the influence of the current intensity on the shape and size of NPs. The electrolysis was conducted at constant current. When the anodic compartment solution is stirred, the NPs formed on the electrode fall down and the electrode surface can be considered unchanged during the process; therefore, the growth speed is directly proportional to the current intensity. In these conditions, the higher the current, the higher the growth speed. At 10 μA, the electrolysis was conducted for 3 days: the morphology of the particles was uniform but their size ranged from 30 to 50 nm. When the current was fixed at 200 μA, the electrolysis was stopped after 3 h 50 min and all particles were in the 50 nm size range. Almost the same size was obtained (55 nm) at a current of 500 μA applied for 1 h 15 min (Figure 3).

Well-dispersed and homogeneous NPs can therefore be readily prepared at currents ranging from 200 and 500 μA. The IR spectrum for the particles grown under these conditions (Figure S6 in the Supporting Information) is identical to that reported previously.[18]

$(TMTSF)_2ClO_4$ Nanoparticles

$(TMTSF)_2ClO_4$ was the first organic superconductor at ambient pressure with a T_c at 1.3 K.[19] As for $(TMTSF)_2PF_6$, NPs of $(TMTSF)_2ClO_4$ have previously been isolated by electrolysis in the presence of the long-chain ammonium salt $[Me(n\text{-}Oct)_3N]ClO_4$, which acts as both the supporting electrolyte and the stabilizer.[2a,18] We have investigated their preparation in the presence of nBu_4NClO_4 or $[Me(n\text{-}Oct)_3N]ClO_4$ as the supporting electrolyte and neutral long-chain molecules as the stabilizers (Table 1, Scheme 3). Except for hexadecylamine, whatever the neutral amphiphilic molecule, TEM micrographs exhibit similar features: nanocrystals with sizes in the 20–70 nm range (Figure 4).

Similar nanocrystals have previously been observed when $(TMTSF)_2ClO_4$ is grown with $[Me(n\text{-}Oct)_3N]ClO_4$ (Figure 5, a).[18] Nevertheless, in the presence of the longer alkyl-chain amine (hexadecylamine), spherical 35 nm diameter nanoparticles were obtained (Figure 5, b). When hexadecylamine was used in combination with $[Me(n\text{-}Oct)_3N]ClO_4$, which also bears a long alkyl chain, smaller spherical NPs were observed together with a few remaining nanocrystals (Figure 5, c). A major improvement results from these conditions: stable dispersions of NPs (ca. 1 d) can be prepared in acetonitrile (2–3 $mg\,mL^{-1}$).

HRTEM measurements performed at 200 kV (Figure 6) indicate that the 20–60 nm features observed in the lower-resolution TEM images from Figure 5a are in fact agglomerates of smaller NPs, with diameters in the 3–5 nm range. The observed interplanar spacings can be indexed in the vast majority of cases according to the well-known $(TMTSF)_2ClO_4$ triclinic crystal structure, thus indicating

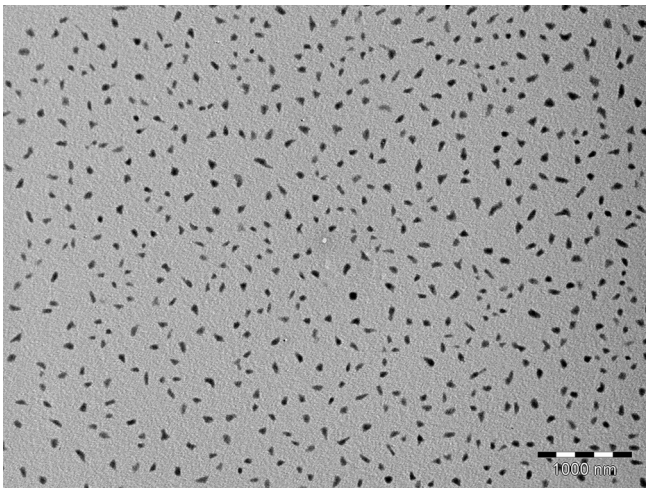

Figure 4. Electron micrographs for $(TMTSF)_2ClO_4$ with octylamine and nBu_4NClO_4; scale bar: 1000 nm.

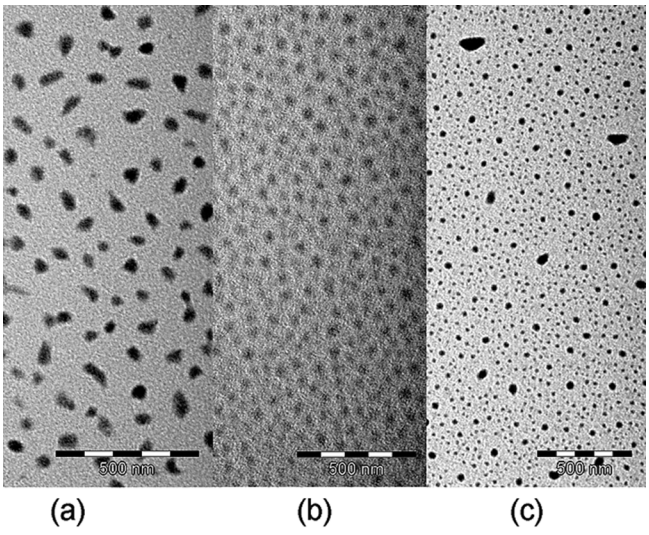

Figure 5. Electron micrographs for $(TMTSF)_2ClO_4$ with (a) $[Me(n\text{-}Oct)_3N]ClO_4$, (b) hexadecylamine and nBu_4NClO_4, and (c) hexadecylamine and $[Me(n\text{-}Oct)_3N]ClO_4$ (all scale bars are 500 nm).

their high degree of order (see also Figure S6 in the Supporting Information).

IR and Raman spectroscopy (see Figures S7 and S8 in the Supporting Information) for the particles grown in this medium are identical to those previously reported.[18]

Figure 7 shows the high-resolution XPS spectra of neutral TMTSF pressed microcrystalline powder (gray line) relative to pressed powder of $(TMTSF)_2ClO_4$ nanoparticles (short dotted line), respectively. The binding energy of the Se $3d_{5/2}$ line that corresponds to neutral TMTSF is located at 55.6 eV after correction of surface charge owing to the insulating character of TMTSF. The Se $3d_{5/2}$–Se $3d_{3/2}$ doublet can be fitted to a mixed Gaussian–Lorentzian function with a full width at half-maximum (FWHM) of 0.9 eV, a branching ratio of 0.83, and a splitting of 0.9 eV after a Shirley-type background subtraction. The Se 3d line that corresponds to $(TMTSF)_2ClO_4$ can be decomposed into

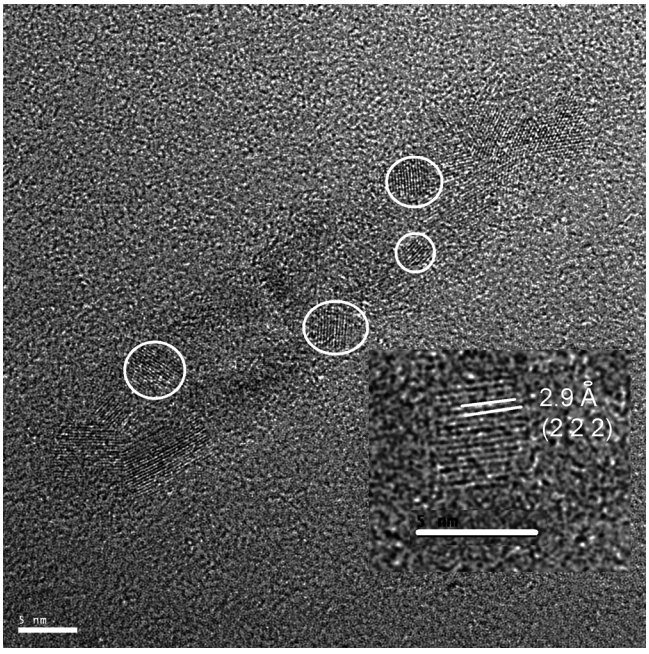

Figure 6. HRTEM image taken at 200 kV of aggregated NPs of $(TMTSF)_2ClO_4$ with $[Me(n\text{-}Oct)_3N]ClO_4$ exhibiting diameters in the 3–5 nm range (scale bar 5 nm). Inset: One indexed 4.5 nm NP.

four contributions (dotted black lines), the sum of which is represented as a black line and mimics the experimental data. In the fit, the values obtained for neutral TMTSF have been taken as fixed parameters to reduce the number of variables. No surface charge was detected, which indicated the conductive character of the powder. The resulting binding energies for the Se $3d_{5/2}$ components are 55.7, 56.1, 57.0, and 58.8 eV, respectively. The first one corresponds to TMTSF in the neutral state, whereas the rest correspond to different oxidation states of TMTSF, thus evidencing charge transfer. The observed energy difference between the first two components, 0.4 eV, is characteristic of related molecules and has been found, for example, in TTF on Au(111) surfaces, which corresponds to a total charge transfer of 0.3 electrons per molecule.[20] The same effect has also been observed for microcrystals of the closely related Fabre salt $(TMTTF)_2PF_6$ (TMTTF = tetramethyltetrathiafulvalene). In this case, two equally intense S 2p components separated by about 1 eV have been reported that correspond to both the neutral and charged (+1) configurations.[21] Analogous S 2p spectra have been obtained for TTF-TCNQ single crystals, with two components separated by approximately 1 eV (about 0.6 charge transfer).[22] The reason for the observation of different configurations is that photoemission is a rapid process (in the 10^{-15} s range). The components associated with the salt appear broader (1.1 eV FWHM) than for TMTSF (0.9 eV FWHM) owing to the small size of the nanoparticles relative to the microcrystalline size of neutral TMTSF. The small size is possibly responsible for the presence of more than two oxidation states (neutral and +1) for $(TMTSF)_2ClO_4$ nanoparticles. However, Raman spectroscopy (Figure S8 in the Supporting Information) evidences the $\nu_4(a_g)$ mode of the central C=C bond of TMTSF at 1461 cm^{-1}, thereby confirming the expected +0.5 formal charge for TMTSF in $(TMTSF)_2ClO_4$.[23]

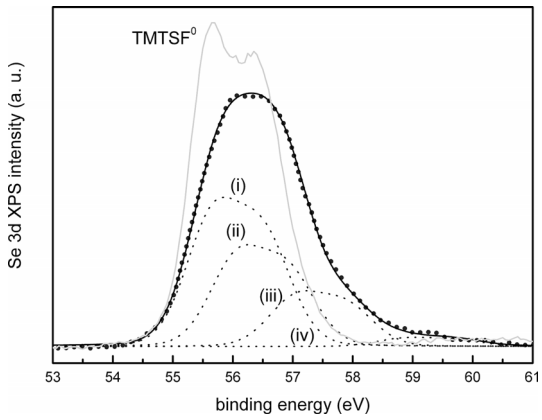

Figure 7. XPS spectra of $(TMTSF)_2ClO_4$ (short dotted line: experimental, black line: calculated) and TMTSF (gray line); the four black dotted lines [from (i) to (iv)] correspond to the deconvolution of the black line (see text for details of the fit).

To measure the superconducting properties of $(TMTSF)_2ClO_4$ NPs, we performed inductive magnetic susceptibility measurements with a tunnel diode oscillator (TDO) (Figure 8). The sample was slow cooled between 40 and 15 K at a rate of approximately 0.05 K min^{-1} to ensure that the anion ordering took place and the material would be in the superconducting state. Afterwards we monitored the frequency from 1.4 to 0.031 K as the dilution refrigerator cooled and warmed, which took about 8.3 h each to complete. Results are shown as a negative frequency owing to frequency change being proportional to the negative change of magnetic susceptibility. As a result, Figure 8 shows a decrease in the negative frequency as the material undergoes the superconducting transition, as expected. The black curve (right axis) is relative susceptibility versus temperature for a bundle of $(TMTSF)_2ClO_4$ crystals[24] that shows

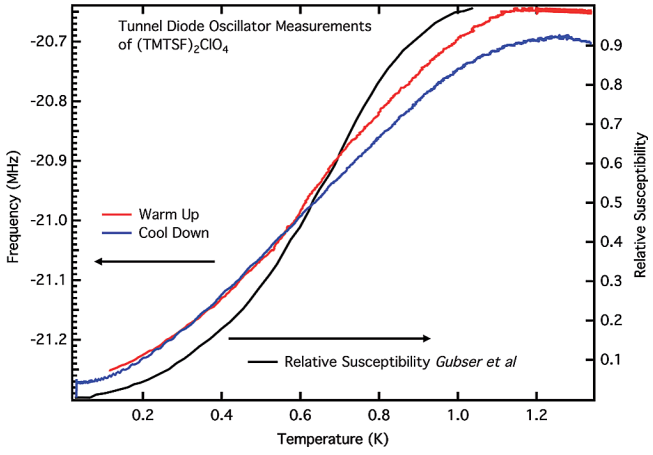

Figure 8. Observation of the superconducting transition of nanoparticles of $(TMTSF)_2ClO_4$ as a function of temperature using a TDO (left axis, blue and red curves).

a similar change in susceptibility through the superconducting transition. Isothermal magnetic field sweeps below T_c (≈1.2 K) show a type-II critical field behavior that is also consistent with the results in the literature.[24] These results will be reported elsewhere.[25]

Conclusion

The preparation of nanoparticles of the four molecular superconductors β-(BEDT-TTF)$_2$I$_3$, TTF[Ni(dmit)$_2$]$_2$, (TMTSF)$_2$PF$_6$, and (TMTSF)$_2$ClO$_4$ was successfully performed under various conditions to fulfill multiple goals: (i) the preparation of new examples of nanoparticles as well-dispersed NPs of β-(BEDT-TTF)$_2$I$_3$ with an average size of 35 nm; (ii) the reduction of the particle size by applying an electrochemical method for growing, at room temperature, 10–15 nm NPs of TTF[Ni(dmit)$_2$]$_2$; (iii) the production of higher amounts of homogeneous particles in shorter amounts of time (1 h versus days) in the case of (TMTSF)$_2$PF$_6$; and (iv) providing evidence of the superconducting transition at low particle size for NPs of (TMTSF)$_2$ClO$_4$. Conditions are now available for isolating these systems as spherical uniform particles, a challenge in the field of molecular conductors and superconductors, which preferably grow as needles. We have additionally provided evidence that spherical crystalline nanoparticles of (TMTSF)$_2$ClO$_4$ as small as 3–5 nm can be formed, organize as 20–60 nm nanocrystals, and exhibit the superconducting transition observed in macroscopic single crystals. Further physical studies of NPs of (TMTSF)$_2$ClO$_4$ and other molecular superconductors are in progress to determine the mechanism that explains the occurrence of superconductivity at such a small size.

Experimental Section

Synthesis: All syntheses were performed at room temperature under an argon atmosphere, except the synthesis of β$_{CO}$-(BEDT-TTF)$_2$I$_3$. Solvents (tetrahydrofuran, acetonitrile, and dichloromethane) were distilled and stored under argon prior to use. BEDT-TTF, TTF, TMTSF, octylamine, dodecylamine, hexadecylamine, methyloleate, *n*Bu$_4$NClO$_4$, and (BMIM)X {X = [N(CF$_3$SO$_2$)$_2$], BF$_4$, PF$_6$} are commercially available and were used as received. [Me(*n*-Oct)$_3$N]-ClO$_4$ and *n*Bu$_4$N[Ni(dmit)$_2$] were prepared as described in the literature.[18,26] *N*-Octylfuran-2-carboxamide and *N*-octylfurfurylimine were prepared following procedures described in the literature.[27]

β$_{CO}$-(BEDT-TTF)$_2$I$_3$ Nanoparticles: BEDT-TTF (100 mg) and (BMIM)[N(CF$_3$SO$_2$)$_2$] (1.5 mL) were dissolved in THF (60 mL). A solution of I$_2$ (99 mg) in THF (20 mL) was added dropwise over 1 h to the first solution heated at 85 °C. The reaction mixture was further cooled to room temperature and for 1 h at 0 °C. A shiny black precipitate (160 mg) was collected by filtration and dried under vacuum for 4 h.

General Conditions of Electrosynthesis of Nanoparticles: The synthesis was performed in a classical H-shaped electrocrystallization cell equipped with two platinum wire electrodes (L = 1 cm, d = 1 mm).[28] The anodic and cathodic compartments were filled with a solution of the selected stabilizing medium (ionic liquid, amine, ammonium salt, from 3 to 10 equiv./TTF or TMTSF) and the appropriate supporting electrolyte. The donor molecule (TTF, TMTSF) was placed in the anodic compartment. The electrolysis was conducted at room temperature under galvanostatic conditions. The anodic solution was vigorously stirred during the entire electrolysis procedure. The air-stable black powders of NPs were collected by filtration from the anodic compartment.

TTF[Ni(dmit)$_2$]$_2$ Nanoparticles: The anodic compartment contained TTF (12 mg), *n*Bu$_4$N[Ni(dmit)$_2$] (81 mg), and (BMIM)[N(CF$_3$SO$_2$)$_2$] or (BMIM)BF$_4$ (90 μL) dissolved in acetonitrile (12 mL). The cathodic compartment contained (BMIM)[N(CF$_3$SO$_2$)$_2$] or (BMIM)BF$_4$ (90 μL) dissolved in acetonitrile (12 mL). The electrolysis was conducted at 150 μA for 24 h in the presence of (BMIM)-BF$_4$ and at 80 μA for 24 h and 500 μA for 4 h in the presence of (BMIM)[N(CF$_3$SO$_2$)$_2$].

(TMTSF)$_2$PF$_6$ Nanoparticles: The anodic compartment contained TMTSF (25 mg), and (BMIM)PF$_6$ (90 mg) dissolved in CH$_2$Cl$_2$ (12 mL). The cathodic compartment contained (BMIM)PF$_6$ (90 mg) dissolved in CH$_2$Cl$_2$ (12 mL). The electrolysis was conducted at different current densities and durations from 10 μA for 3 d to 500 μA for 1 h 15 min.

(TMTSF)$_2$ClO$_4$ Nanoparticles: The anodic compartment contained TMTSF (25 mg) and *n*Bu$_4$NClO$_4$ (80 mg) or [Me(*n*-Oct)$_3$N]ClO$_4$ (105 mg) dissolved in solvent (CH$_2$Cl$_2$ or THF, 12 mL). The cathodic compartment contained *n*Bu$_4$NClO$_4$ (75 mg) or [Me(*n*-Oct)$_3$-N]ClO$_4$ (105 mg) dissolved in solvent (12 mL). The following amphiphilic molecules were added to the anodic compartment: hexadecylamine (32 mg), dodecylamine (25 mg), *n*-octylamine (74 μL), methyloleate (65 μL), *N*-octylfuran-2-carboxamide (37 mg), or *N*-octylfurfurylimine (37 μL). Currents and durations of electrolysis are indicated in Table 1.

Physical Measurements: TEM experiments were performed with a JEOL model JEM 1011 operating at 100 kV. The powder (0.5 mg) was dispersed in diethyl ether (2 mL) under slow stirring for 1 min. The TEM specimen was then prepared by evaporation of droplets of suspension deposited on carbon-supported copper grids.

HRTEM images were recorded with an FEI Tecnai F20 HRTEM operating at 200 kV. The samples were sonicated, dispersed in acetonitrile, and placed dropwise onto a holey carbon–copper support grid for HRTEM observation.

Ex situ XPS experiments were performed at room temperature with a SPECS PHOIBOS 150 hemispherical analyzer at 10 eV pass energy using monochromatic Al-K_α (1486.6 eV) radiation as excitation source at a base pressure of 10^{-9} mbar.

The tunnel diode oscillator (TDO) technique consists of an LC tank circuit that oscillates at its resonant frequency, $f_0 = [2\pi\sqrt{(LC)}]^{1/2}$, and a tunnel diode that compensates for losses in the circuit. The sample to be studied went inside the inductor (L) coil and we monitored the change in frequency as a function of temperature and field. As the magnetic properties of the material change, the effective inductance of the coil changes and therefore the resonant frequency of the circuit changes, which we used as a measure of the magnetic susceptibility changes of the sample. In our experiment, we packed the (TMTSF)$_2$ClO$_4$ NPs (7.385 mg) inside a plastic nonmagnetic capsule, which had an approximate volume of 22.51 mm^3. The capsule was then placed inside a 40 turn (L) coil of about 4.66 mm length with an approximate volume of 26.73 mm^3. The resonant frequency was around 15 MHz and was mixed with a local 5 MHz frequency source to obtain the 20–21 MHz results presented in Figure 8. The experiment was run in

a dilution refrigerator in which temperature sweeps were carried out between 35 mK and 1.2 K, with a field range of –2 to 2 T provided by a superconducting magnet.

Supporting Information (see footnote on the first page of this article): Raman spectra, infrared spectra, X-ray diffraction data, and HRTEM data.

Acknowledgments

Work done at the National High Magnetic Field Laboratory (NHMFL) was supported by the National Science Foundation (NSF) (DMR-1309146) (grant to J. S. B). The NHMFL was supported by the NSF Cooperative, Agreement Number DMR-1157490, the State of Florida, and the U.S. Department of Energy. Collaboration within the European Associated Laboratory Trans-Pyrénéen (LEA) (program: "de la Molécule aux Matériaux") is appreciated. Work done at the Laboratoire de Chimie de Coordination (LCC) was supported by the French Centre National de la Recherche Scientifique (CNRS). I. C. thanks the French Ministère de l'Enseignement Supérieur et de la Recherche (MESR) for a Ph.D. grant.

[1] L. Valade, H. Tanaka, in: *Molecular Materials* (Eds.: D. W. Bruce, R. Walton), Wiley, **2010**, p. 215–290.

[2] a) D. de Caro, L. Valade, C. Faulmann, K. Jacob, D. Van Dorsselaer, I. Chtioui, L. Salmon, A. Sabbar, S. El Hajjaji, E. Perez, S. Franceschi, J. Fraxedas, *New J. Chem.* **2013**, *37*, 3331–3336; b) T. Kadoya, D. de Caro, K. Jacob, C. Faulmann, L. Valade, T. Mori, *J. Mater. Chem.* **2011**, *21*, 18421–18424.

[3] E. Laukhina, J. Ulanski, A. Khomenko, S. Pesotskii, V. Tkatchev, L. Atovmyan, E. Yagubskii, C. Rovira, J. Veciana, J. Vidal-Gancedo, V. Laukhin, *J. Phys. I* **1997**, *7*, 1665–1675.

[4] J. P. Savy, D. De Caro, L. Valade, J. P. Legros, P. Auban-Senzier, C. R. Pasquier, J. Fraxedas, F. Senocq, *Europhys. Lett.* **2007**, *78*.

[5] J.-P. Savy, D. de Caro, L. Valade, J.-C. Coiffic, E. S. Choi, J. S. Brooks, J. Fraxedas, *Synth. Met.* **2010**, *160*, 855–858.

[6] E. E. Laukhina, V. A. Merzhanov, S. I. Pesotskii, A. G. Khomenko, E. B. Yagubskii, J. Ulanski, M. Kryszewski, J. K. Jeszka, *Synth. Met.* **1995**, *70*, 797–800.

[7] D. de Caro, M. Souque, C. Faulmann, Y. Coppel, L. Valade, J. Fraxedas, O. Vendier, F. Courtade, *Langmuir* **2013**, *29*, 8983–8988.

[8] M. Mas-Torrent, E. E. Laukhina, V. Laukhin, C. M. Creely, D. V. Petrov, C. Rovira, J. Veciana, *J. Mater. Chem.* **2006**, *16*, 543–545.

[9] a) E. É. Kostyuchenko, É. B. Yagubskii, O. Y. Neiland, V. Y. Khodorkovskii, *Russ. Chem. Bull.* **1984**, *33*, 2598; b) E. E. Laukhina, V. N. Laukhin, A. G. Khomenko, E. B. Yagubskii, *Synth. Met.* **1989**, *32*, 381–388; c) H. Müller, S. O. Svensson, A. N. Fitch, M. Lorenzen, D. G. Xenikos, *Adv. Mater.* **1997**, *9*, 896–900.

[10] R. P. Shibaeva, E. B. Yagubskii, *Chem. Rev.* **2004**, *104*, 5347–5378.

[11] E. B. Yagubskii, I. F. Shchegolev, V. N. Laukhin, P. A. Kononovich, M. V. Karatsovnik, A. V. Zvarykina, L. I. Buravov, *Jetp Lett.* **1984**, *39*, 12–16.

[12] A. Tracz, J. K. Jeszka, A. Sroczynska, J. Ulanski, T. Pakula, *Adv. Mater. Opt. Electronics* **1996**, *6*, 335–342.

[13] A. Funabiki, H. Sugiyama, T. Mochida, K. Ichimura, T. Okubo, K. Furukawa, T. Nakamura, *Rsc Adv.* **2012**, *2*, 1055–1060.

[14] L. Brossard, M. Ribault, M. Bousseau, L. Valade, P. Cassoux, *C. R. Acad. Sci.* **1986**, *302-II*, 205–210.

[15] W. Kaddour, P. Auban-Senzier, C. Pasquier, L. Valade, *Phys. B* **2012**, *407*, 1715–1717.

[16] a) D. de Caro, J. Fraxedas, C. Faulmann, I. Malfant, J. Milon, J. F. Lamère, V. Collière, L. Valade, *Adv. Mater.* **2004**, *16*, 835–838; b) D. de Caro, K. Jacob, C. Faulmann, L. Valade, L. Viau, *C. R. Chim.* **2012**, *15*, 950–954.

[17] D. Jérome, A. Mazaud, M. Ribault, K. Bechgaard, *J. Physique Lett.* **1980**, *41*, 95–98.

[18] D. de Caro, K. Jacob, C. Faulmann, L. Valade, *C. R. Chim.* **2013**, *16*, 629–633.

[19] K. Bechgaard, K. Carneiro, F. B. Rasmussen, M. Olsen, G. Rindorf, C. S. Jacobsen, H. J. Pedersen, J. C. Scott, *J. Am. Chem. Soc.* **1981**, *103*, 2440–2442.

[20] a) I. Fernandez-Torrente, S. Monturet, K. J. Franke, J. Fraxedas, N. Lorente, J. I. Pascual, *Phys. Rev. Lett.* **2007**, *99*, 176103/1–176103/4; b) J. Fraxedas, S. Garcia-Gil, S. Monturet, N. Lorente, I. Fernandez-Torrente, K. J. Franke, J. I. Pascual, A. Vollmer, R. P. Blum, N. Koch, P. Ordejon, *J. Phys. Chem. C* **2011**, *115*, 18640–18648.

[21] a) J. Fraxedas, *Molecular Organic Materials: From Molecules to Crystalline Solids*, Cambridge University Press, Cambridge, UK, **2006**; b) G. Subias, T. Abbaz, J. M. Fabre, J. Fraxedas, *Phys. Rev. B* **2007**, *76*, 085103/1–085103/7.

[22] a) J. Fraxedas, Y. J. Lee, I. Jimenez, R. Gago, R. M. Nieminen, P. Ordejon, E. Canadell, *Phys. Rev. B* **2003**, *68*, 195115/1–195115/11; b) M. Sing, U. Schwingenschlogl, R. Claessen, M. Dressel, C. S. Jacobsen, *Phys. Rev. B* **2003**, *67*, 125402/1–125402/11.

[23] R. Bozio, C. Pecile, K. Bechgaard, F. Wudl, D. Nalewajek, *Solid State Commun.* **1982**, *41*, 905–910.

[24] D. U. Gubser, W. W. Fuller, T. O. Poehler, D. O. Cowan, M. Lee, R. S. Potember, L. Y. Chiang, A. N. Bloch, *Phys. Rev. B* **1981**, *24*, 478–480.

[25] L. E. Winter, E. S. Steven, J. S. Brooks, D. de Caro, C. Faulmann, L. Valade, K. Jacob, I. Chtioui, J. Fraxedas, B. Ballesteros, unpublished results.

[26] G. Steimecke, H.-J. Sieler, R. Kirmse, E. Hoyer, *Phosphorus Sulfur Relat. Elem.* **1979**, *7*, 49–55.

[27] M. Bergez-Lacoste, S. Thiebaud-Roux, P. de Caro, J.-F. Fabre, Z. Mouloungu, *Dérivés du furfural pour une application biosolvants*, patent FR1351811, France, **2013**.

[28] a) P. Cassoux, L. Valade, P.-L. Fabre, in: *Comprehensive Coordination Chemistry II: From Biology to Nanotechnology, Fundamentals: Ligands, Complexes, Synthesis Purification and Structure*, vol. 1 (Ed.: A. B. P. Lever), Elsevier, Amsterdam, **2003**, p. 761–773; b) P. Batail, K. Boubekeur, M. Fourmigué, J.-C. P. Gabriel, *Chem. Mater.* **1998**, *10*, 3005–3015.